

PAPER

Iridescent cellulose nanocrystal films: the link between structural colour and Bragg's law

To cite this article: Thanh-Dinh Nguyen *et al* 2018 *Eur. J. Phys.* **39** 045803

View the [article online](#) for updates and enhancements.

Related content

- [Photonic-structured fibers assembled from cellulose nanocrystals with tunable polarized selective reflection](#)
Xin Meng, Hui Pan, Tao Lu *et al.*
- [Functional materials based on nanocrystalline cellulose](#)
Oleg V. Surov, Marina I. Voronova and Anatoly G. Zakharov
- [An optical study of the structure of the helicoidal twist grain boundary \(TGB_x\) phase](#)
Richard J Miller, Helen F Gleeson and John E Lydon

Recent citations

- [Teflon tape for laboratory teaching of three-dimensional x-ray crystallography](#)
Aitor Larrañaga *et al*




IOP | ebooks™

Bringing you innovative digital publishing with leading voices to create your essential collection of books in STEM research.

Start exploring the collection - download the first chapter of every title for free.

Iridescent cellulose nanocrystal films: the link between structural colour and Bragg's law

Thanh-Dinh Nguyen¹, Egoitz Sierra²,
Harkaitz Guirraun^{2,3} and Erlantz Lizundia^{2,4} 

¹ Department of Chemistry, University of British Columbia, Vancouver, British Columbia, V6T 1Z1, Canada

² Department of Graphic Design and Engineering Projects, Bilbao Faculty of Engineering, University of the Basque Country (UPV/EHU), Bilbao E-48103, Spain

³ Research Center for Experimental Marine Biology and Biotechnology-Plentziako Itsas Estazioa (PiE), University of the Basque Country (UPV/EHU), Plentzia E-48620, Spain

⁴ BCMaterials, Parque Científico y Tecnológico de Bizkaia, E-48160 Derio, Spain

E-mail: erlantz.liizundia@ehu.eus

Received 1 February 2018, revised 2 March 2018

Accepted for publication 9 March 2018

Published 30 April 2018



CrossMark

Abstract

Structural colour is a phenomenon found in nature, which provides plants and animals with vibrant optical properties. The production of this colour is based on the interaction of incident light with the hierarchical organisation of sub-micron- and micron-sized layered structures. Cellulose nanocrystals (CNCs) are anisotropic building units formed by acid hydrolysis of native cellulose microfibrils, which can disperse in aqueous media to form a photonic liquid crystal. One fascinating example of the appearance of biomimetic colour is the supramolecular assembly of CNCs into iridescent layered structures that rotate along a helical screw to yield a long-range chiral nematic order. A quick, simple and engaging experiment that allows the establishment of a direct relation between the structural colour and underlying mechanism of the light interaction with these hierarchically structured materials is reported. The obtained colour changes are explained within the theoretical framework provided by Bragg's law and may provide an easy way to observe the macroscopic manifestation of this often abstract concept.

Keywords: Bragg's law, structural colour, photonics, chirality, physical properties

(Some figures may appear in colour only in the online journal)

1. Introduction

Many living organisms use colour for functions such as signalling, physiological regulation or camouflage [1]. In the present *Journal* and as far as we are aware, there exist many physics experiments especially designed for undergraduate courses which are focused on different aspects related to colour [2–7]. In contrast, we found very few works focused on structural colour, which is an exciting area of study in photonics.

Structural colour refers to the production of colour by hierarchically arranged structures. These naturally occurring periodic structures usually display a layered architecture. In some cases they also present a chiral nematic organisation due to their internal organisation at the nanoscale level. These structures are able to interact with light to provide materials with photonic properties. For instance, the blue iridescence of the *Pollia condensata* fruit (Marble berry) and the blue-green iridescence of the *Mapania caudata* leaves arise from the presence of a periodic structure, a helicoidal stacking of cellulose [8, 9]. Similarly, the brilliant colour of jewel beetle exoskeletons has been reported to arise from a chiral periodic structure composed of chitin [10].

These naturally occurring architectures are made up by helical assemblies, which can be organised into left-handed or right-handed structures, defining the handedness or helicity of the material. Since this property determines the manner in which the chiral structure interacts with its surroundings [11], it plays a pivotal role in disciplines linked with physics, chemistry and biology. To that end, several works have been devoted to the teaching of physics related to colours, liquid crystals and similar materials. For instance, the temperature susceptibility of a cholesteric liquid crystal has proved to be useful for the teaching of the existing relationship between assembled structure and the reflected/transmitted colours as the distance between successive layers increases with temperature [12]. In addition, the formation of birefringence patterns under everyday conditions has also been discussed in this *Journal* for general optics courses [7], and the quantitative determination of the anisotropic optical properties of polymers useful for students of specialised physics and engineering has also been discussed [6]. Furthermore, these experiments based on materials having helical chiral nematic order, represent plausible approaches for the teaching of colours and related physical aspects. We believe there is a lack of works connecting natural colours with their hierarchically arranged structure and their link with the theoretical framework provided by Bragg's law, a special case of Laue diffraction.

In addition, students find chirality a challenging topic because it involves the visualisation of 3D nanoscale-level structures, which is not easy to imagine through textbooks [13]. Although several laboratory experiments have been devoted to allowing an easier understanding of the underlying phenomena of molecular chirality by approaches such as polarimetry [14, 15], to date these approaches have not provided palpable evidence on the concept of chirality and colour and their presence in all aspects of nature.

The novelty of this work is that we provide a simple and safe experiment, which enables students to connect the abstract ideas of hierarchical organisation and chirality to the physical phenomena of structural colour often found in nature. This experiment offers the opportunity to observe the existing structure-property link by simply visualising how the change of the ordered structure of a material is able to modify its interaction with light, which is explained within the theoretical framework of Bragg's law. Indeed, students would confront the experimental measurement of helical pitch in hierarchically arranged materials using several laboratory techniques with the reflected light, observable with the naked eye. Finally, this experiment serves as a novel way to successfully integrate materials science into general physics teaching [16].

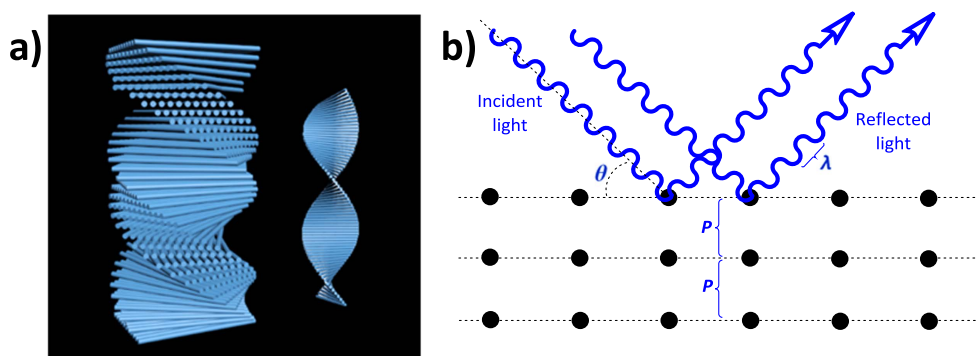


Figure 1. Scheme (a) showing the hierarchical organisation of chiral nematic CNC films and the relationship of P helical pitch with reflected light (b).

2. Theoretical background

This experiment is designed to create an understanding of the relationship between the hierarchical organisation of materials and their interaction with light using cellulose nanocrystals (CNCs). CNCs are a new type of nanomaterial, which presents a rod-like aspect [17–19], and could be obtained via the controlled disintegration of cellulose. Under suitable conditions, CNCs are able to organise into a characteristic long-range chiral nematic order [20, 21]. These twisted layers resemble crystal lattices, which under certain circumstances are able to lead to a phenomenon known as Bragg's diffraction. This diffraction occurs when radiation having a wavelength comparable to successive crystallographic planes is scattered by different lattice planes that remain separated by the d interplanar distance. Therefore, depending on the wavelength of the incident wave (λ), these scattered waves are able to interfere constructively according to Bragg's law:

$$2d \sin(\theta) = m\lambda \quad (1)$$

where m is a positive integer ($m = 1, 2, \dots$) and θ is the scattering angle. m integer ensures a constructive interference of reflected waves. Within this framework and following equation (1), the pitch of the helix formed by the self-assembly of cellulose nanocrystals, often referred to as P , determines the colour of the resulting film and is computed as

$$\lambda_{\max} = n_{\text{avg}} P \sin(\theta) \quad (2)$$

where λ_{\max} is the reflected light wavelength, θ is the angle of the incident light and n_{avg} is the average refractive index of the material [22, 23]. According to equation (2), the colour of the films could be simply tuned by modulating both the repeating distance between the twisted CNC layers or the refractive index of the material [20]. As shown in figure 1, the structural colour arising from the CNC assemblies with chiral nematic ordering can be seen as a useful property to highlight the effect of the interplanar spacing on the photonic activities of hierarchical ordered structures.

Furthermore, and thanks to the chiral nematic organisation of CNCs, these structures are able to selectively reflect the incident light. This light is circularly polarised into a handedness that matches the handedness of the phase (the twist sense of the helix). Since CNCs are oriented in an anti-clockwise direction through the film, the reflected light is left-handed circularly polarised. Thus, the polarisation of reflected light could be used to provide a reliable evidence of the chiral order of colourful CNC films [24].

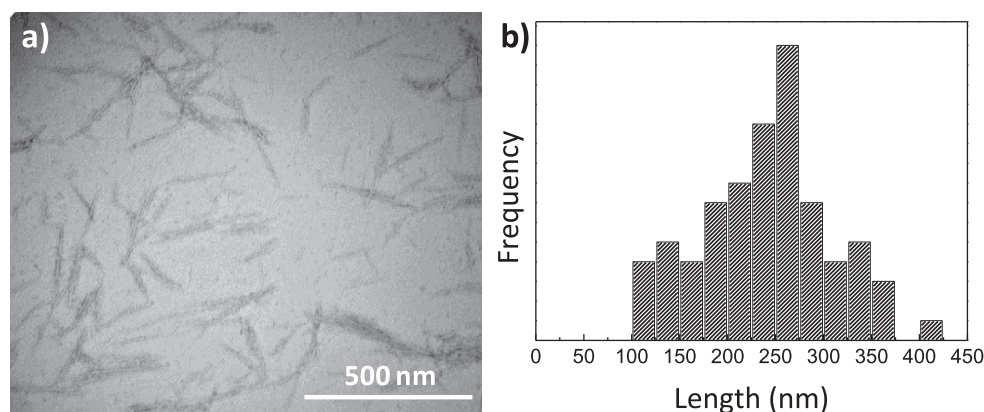


Figure 2. (a) Representative TEM showing CNC morphology and (b) CNC length distribution based on a count of 80 particles.

3. Experimental setup

3.1. Starting materials

The following raw materials are required for the successful development of the experiment. Commercial Kraft softwood pulp can be obtained from CelluForce Inc. Sulphuric acid (CAS Number: 7664-93-9) and ethanol (CAS Number: 64-17-5) are analytical grade reagents from Sigma Aldrich and can be used as received without further purification. For the synthesis of chiral nematic CNC films, no special equipment is required beyond a fume hood, common laboratory equipment (heating and stirring plate) and safety goggles, gloves and lab attire. All these chemical reagents are rather common in laboratories and can be obtained at an affordable price.

3.2. Synthesis of CNCs

One of the most common techniques to obtain CNCs is their controlled degradation using acids. This procedure allows the removal of the amorphous parts in the native cellulose to give short rod-like fibrils of high crystallinity with nanometric size. After the acidic attack, the resulting dispersion needs to be washed several times to remove dissolved impurities and excess acid, so that pure CNC nanoparticles can be obtained.

Accordingly, for this work CNCs are synthesised by sulphuric acid hydrolysis of fully-bleached commercial Kraft softwood pulp [25–27]. A milled softwood pulp is submitted to sulphuric acid hydrolysis at a concentration of 64% by weight (sulphuric acid to deionised water) and a temperature of 45 °C under mild magnetic stirring for 25 min. The suspension is then diluted tenfold with cold deionised water to quench the reaction, and the excess acid is then removed by decantation, centrifugation (4000 rpm for 15 min) and dialysis using bags with a molecular weight-cut-off of 12–14,000 Da. Finally, the resulting dispersion is submitted to an ultrasound treatment in a Fisher Sonic Dismembrator (Fisher Scientific) for 10 min at 60% power to obtain a CNC dispersion of 4.2% by weight with a pH of 2.5.

The morphology of the obtained nanometric-sized cellulosic nanoparticles can be observed under the transmission electron microscopy (TEM) image in figure 2(a) (Hitachi H7600 microscope). As shown in figure 2(b), these CNCs consist of 240 ± 62 nm long and 10 nm wide nanoparticles (length distribution is based on a count of 80 particles). Similarly,

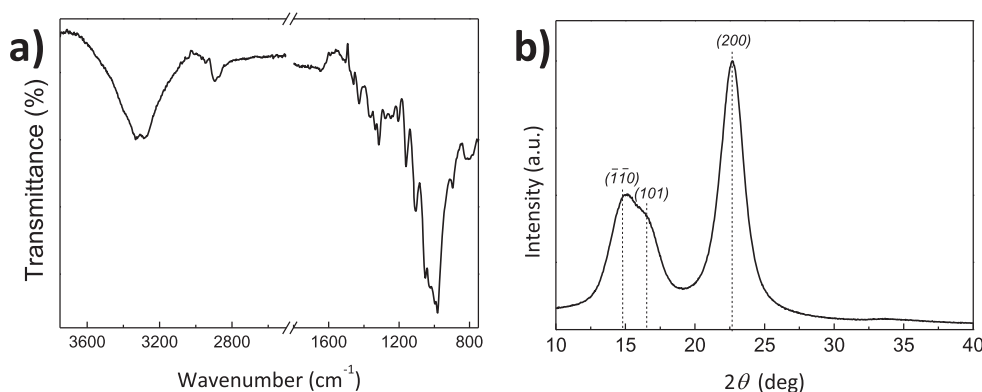


Figure 3. (a) FTIR spectra and (b) PXRD pattern of CNC film.

the chemical structure of the synthesised CNCs is also analysed under Fourier transform infrared spectroscopy (Nicolet 6700 FTIR equipped with a smart orbit diamond attenuated total reflectance attachment) and x-ray diffraction (D8 Advance x-ray diffractometer with $\lambda = 1.540 \text{ \AA}$) in figure 3. The obtained FTIR spectra present the characteristic peaks of cellulose at 3650–3200, 2902, 1337, 1160 and 897 cm^{-1} (corresponding to the O–H stretching vibration, asymmetric C–H stretching vibration, C–O–H bending, C–O–C bending and the C–O–C asymmetric stretching at the β -(1 \rightarrow 4)-glycosidic linkage) [28]. Moreover, the crystalline structure of CNCs can be analysed by powder x-ray diffraction (PXRD), where the pattern in figure 3(b) presents three main peaks centred at $2\theta = 14.9^\circ$, 16.5° and 22.7° confirming that CNCs are composed of cellulose I [29, 30]. These two experiments are performed to check that the structure of the cellulose is not modified during the sulphuric acid attack.

3.3. Preparation of chiral nematic CNC films

Free-standing 50 μm thick chiral nematic CNC films are obtained by evaporation-induced self-assembly (EISA) of a CNC suspension. 12 ml of aqueous CNC dispersion (4.2 wt.%, pH = 2.5) are ultrasonicated for 10 min at room temperature and then cast on a polystyrene Petri dish (90 mm diameter). The dispersion is then allowed to dry under ambient conditions for 96 h. The CNC film morphology is characterised by scanning electron microscopy (SEM, Hitachi S4700) in figure 4. The cross-section of a CNC film was attached to an aluminium stub using double-sided adhesive tape and then sputter coated with gold–palladium (5 nm thick layer). The CNC film shows the characteristic features corresponding to the long-range chiral nematic structure, where the repeated distance between the twisted layers (also known as the helical pitch) is about several hundred nanometres [26].

3.4. Hazards

It is obligatory to use goggles, gloves and appropriate lab attire during the entire experiment. Concentrated sulphuric acid, being corrosive and oxidising, can produce hazardous fumes, cause chemical burns and thus should be handled in a well-ventilated fume hood. Ethanol is flammable and should be kept away from ignition sources. It is also an irritant to the skin, eyes and respiratory system, and contact with skin should be avoided. Accordingly, CNC

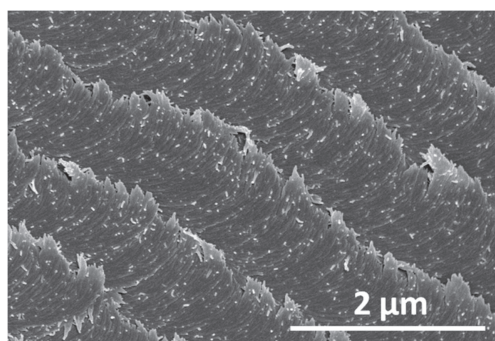


Figure 4. SEM micrograph of the CNC film viewed along the fractural cross-section with the chiral nematic axis perpendicular to the top surface. The relationship of the obtained layered structure can be seen with the scheme provided in figure 1.

synthesis must be conducted in a fume hood. Waste materials should be disposed of in suitably marked containers available in fume hoods.

3.5. Sample characterisation procedure

The experimental characterisation here reported is relatively quick and can be accomplished in a single laboratory session consisting of 2 h. Once free-standing chiral nematic CNC films are fabricated following the instructions given in section 3.3, this experiment only requires simple photonic characterisation and the preparation of several ethanol/water mixtures in order to be able to explain the macroscopic manifestation of Bragg's law. The use of ethanol/water mixtures allows obtaining the media which induces different swelling of the films, but also presents the same refractive index as the selected solvents that present similar refractive indexes. Accordingly, the interference between the solvent and light is avoided.

First of all, the optical properties of the fabricated CNC films are evaluated using ultraviolet-visible spectroscopy (UV-vis) in transmittance mode. A dried CNC is placed between two glass slides and is introduced into the UV-vis chamber to observe the maximum of the reflected wavelength and link this wavelength with its colour that can be observed with the naked eye. This can be carried out using a Cary 5000 UV-vis spectrophotometer. Similarly, the same film is observed under circular dichroism (CD) spectroscopy, which enables the determination of the 'handedness' of the sample as it involves circularly polarised light, i.e. the differential absorption between right- and left-handed light is recorded. A JASCO J-710 spectropolarimeter is used to that end. Subsequently, CNC films are observed under polarised optical microscopy (POM) using an Olympus BX41 microscope, which allows the examination of the microstructure of the films.

Then, 100/0, 75/25, 50/50, 25/75 and 0/100 ethanol/water solvent mixtures of 10 ml should be prepared in different vials. Film pieces ($2 \times 2 \text{ cm}^2$) are simply placed onto a glass slide using tweezers and several solvent mixture drops are added onto these films. As previously done for the dried films, the UV-vis and CD properties of the swollen films are again measured (note that for UV-vis and CD spectroscopy measurements another glass slide should be placed on the sample in order to sandwich the sample between two glass slides). The students are again required to observe these soaked films under POM and measure the P and calculate the interplanar distance (helical pitch) according to Bragg's law. The latter CNC films are allowed to dry.

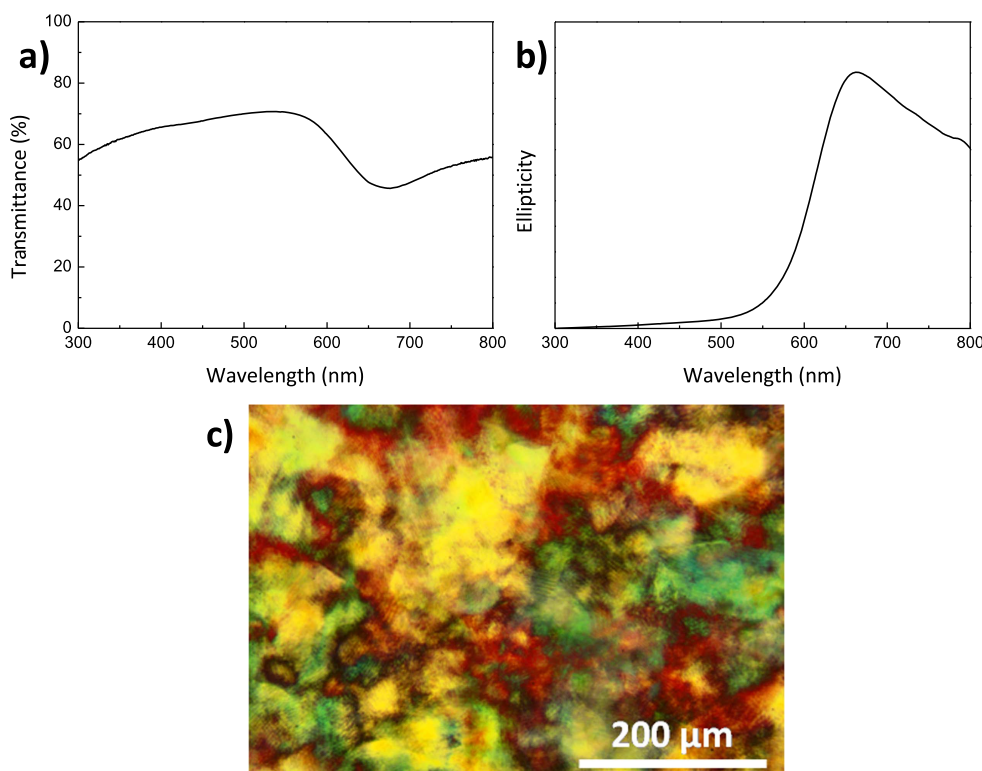


Figure 5. Optical properties of films: (a) UV–vis spectrum, (b) CD spectrum and (c) POM image.

4. Results and discussion

It is observed in figures 5(a) and (b) that the CNC film reflectance peak found in the UV–vis spectra matches the maximum CD signal located at about 660 nm. This wavelength corresponds to orange-red colour, which corresponds to the macroscopic appearance of the film. In addition, the CD spectrum in figure 5(b) displays an intense signal with positive ellipticity, implying a left-handed chiral nematic order [31]. The POM image in figure 5(c) reveals a characteristic fingerprint texture observed in many chiral nematic phases. The helical pitch of the films could be measured from such optical microscopy images and Bragg's law could be applied to determine the theoretically reflected wavelength of the film and compare the value obtained from the UV–vis and CD characterisation.

Once the structural and optical properties are determined and their relationship is explained in terms of Bragg's law, students could be asked to predict what would happen if these iridescent CNC films are soaked with different solvents. When CNC films are immersed in different solvents, their colour is rapidly changed (figures 6(a)–(c)). Indeed, depending on the ethanol/water ratio, the film colour is tailored across the whole visible spectrum [32, 33].

The class is then asked to explain this finding and is prompted to theoretically link the obtained changes with the structure of the films (Bragg reflection of visible light). Photographs of obtained changes are given in figures 6(b) and (c). Notably, the solution of pure

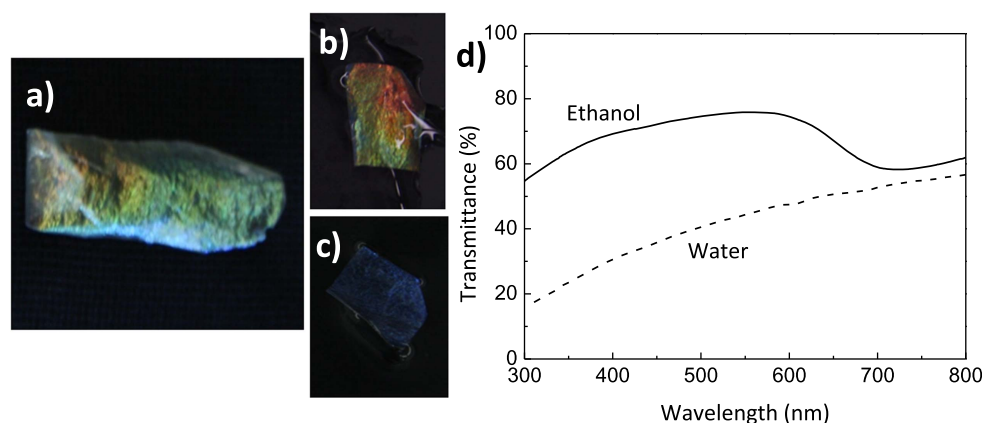


Figure 6. Soaking of iridescent dried CNC films (a) in pure ethanol (b) and pure water (c). Corresponding UV–vis spectra (d).

water induces the greater colour changes because the films swell to the greatest extent in pure water [32]. UV–vis and CD properties of swollen films are shown in figure 6(d), where with an increase in the amount of ethanol, the red-shift of reflected light is notably smaller. Indeed, the film colour varies over the whole visible spectrum from cyan to red and even to transparent for wavelengths exceeding 800 nm. The students are then asked to calculate the interplanar distance (helical pitch) according to Bragg's law and the observed coloration changes. They would observe that the helical pitch depends on the ethanol/water ratio. After the CNC films are allowed to dry, the original colour is recovered, indicating that the observed changes are reversible. In as little as 20 min, this experiment could provide a convincing visual proof of how the structure affects the macroscopic properties of the materials.

At this point, students could get enough data to correlate the implications of Bragg's law with the light interaction and diffraction. If the required experimental techniques are not available, the experiment here proposed could be modified in several ways to accommodate the available resources. CNC films could be simply soaked in variable ethanol/water mixtures and observe their colour change with the naked eye (without the use of UV–vis or CD spectroscopy). It is observed that the swelling of the CNC film induces a greater distance between successive planes (helical pitch) and increases the wavelength of reflected light in the visible region, and thus the film colour.

An expanded version of this experiment and a further step in explaining the interaction of light with hierarchically ordered structures could deal with the chirality of the films by using circular polarisers. Dry or soaked CNC films could also be observed through left-handed and right-handed circular polarisers, which could be obtained from simple disposable cinema 3D movie glasses, which use polarising glasses to create 3D images by restricting the light that reaches each eye. This would enable a simple test for directly visualising the circularly polarised light arising from the CNC films. It is observed that reflected light could only be seen through the left circular filter in the 3D movie glasses, indicating that the CNC helix is oriented into a left-handed structure (figure 7).



Figure 7. Observation of two CNC films through the two different lenses of 3D glasses (left-handed and right-handed circular polarisers).

5. Conclusions

The design of this work provides an effective experiment to understand the existing relationship between hierarchical organisation, structural colour and Bragg's law using cellulose nanocrystals. It also serves to introduce students to basic spectroscopy methods such as UV–vis spectroscopy and POM, which are a core part of the curriculum in areas including physics, chemistry and biology and can be found in many laboratories [25]. The abstract concept of chirality is satisfactorily introduced owing to the characteristic chiral nematic structure of CNCs that could be easily realised by quickly observing disposable 3D movie glasses. The use of laboratory equipment to measure and manipulate iridescent films that change their colour permits a better understanding of the macroscopic implications of Bragg's law. Analogies with plants and animals such as peacock tail feathers and European bee-eaters as naturally occurring hierarchical structures could also be introduced to facilitate the learning of these new biomimetic concepts.

Acknowledgments

Erlantz Lizundia gratefully acknowledges Wadood Y Hamad and Mark J MacLachlan for their assistance, comments, and support.

ORCID iDs

Erlantz Lizundia  <https://orcid.org/0000-0003-4013-2721>

References

- [1] Stuart-Fox D and Moussalli A 2009 Camouflage, communication and thermoregulation: lessons from colour changing organisms *Philos. Trans. R. Soc. Lond. B. Biol. Sci.* **364** 463–70
- [2] Babi V and Epi M 2009 Complementary colours for a physicist *Eur. J. Phys.* **30** 793–806
- [3] Haußmann A 2016 Rainbows in nature: recent advances in observation and theory *Eur. J. Phys.* **37** 063001
- [4] Pavlin J, Vaupotič N and Čepič M 2013 Liquid crystals: a new topic in physics for undergraduates *Eur. J. Phys.* **34** 745–61
- [5] Rodríguez I, Ramiro-Manzano F, Meseguer F and Bonet E 2011 Fabrication and characterization of colloidal crystal thin films *Eur. J. Phys.* **32** 505–15

- [6] Sinyavsky N and Korneva I 2017 Polarimetric study of the optical anisotropy of polymers *Eur. J. Phys.* **38** 045301
- [7] Zhang Y, Chen L, Wang S and Zhou H 2014 Formation of birefringence patterns under everyday conditions *Eur. J. Phys.* **35** 055008
- [8] Vignolini S, Rudall P J, Rowland A V, Reed A, Moyroud E, Faden R B, Baumberg J J, Glover B J and Steiner U 2012 Pointillist structural color in Pollia fruit *Proc. Natl Acad. Sci.* **109** 15712–5
- [9] Strout G, Russell S D, Pulsifer D P, Erten S, Lakhtakia A and Lee D W 2013 Silica nanoparticles aid in structural leaf coloration in the Malaysian tropical rainforest understory herb *Mapania caudata* *Ann. Bot.* **112** 1141–8
- [10] Sharma V, Crne M, Park J O and Srinivasarao M 2009 Structural origin of circularly polarized iridescence in jeweled beetles *Science* **325** 449–51
- [11] Chen Z, Wang Q, Wu X, Li Z and Jiang Y-B 2015 Optical chirality sensing using macrocycles, synthetic and supramolecular oligomers/polymers, and nanoparticle based sensors *Chem. Soc. Rev.* **44** 4249–63
- [12] Lisensky G, Boatman E and College B 2005 Colors in liquid crystals *J. Chem. Educ.* **82** 1360A – 1360B
- [13] Cody J A, Craig P A, Loudermilk A D, Yacci P M, Frisco S L and Milillo J R 2012 Design and implementation of a self-directed stereochemistry lesson using embedded virtual three-dimensional images in a portable document format *J. Chem. Educ.* **89** 29–33
- [14] Vaksman M A and Lane J W 2001 Using guided inquiry to study optical activity and optical rotatory dispersion in a cross-disciplinary chemistry lab *J. Chem. Educ.* **78** 1507
- [15] Kelly C O, Mosher M W and Mosher M D 1996 Examination of a reaction mechanism by polarimetry: an experiment for the undergraduate organic chemistry laboratory *J. Chem. Educ.* **73** 567
- [16] Moore J W and Stanitski C L 2017 Lengthening the chain: polymers in general chemistry *J. Chem. Educ.* **94** 1603–6
- [17] Marchessault F F, Morehead F F and Walter N M 1959 Liquid crystal systems from fibrillar polysaccharides *Nature* **184** 632–3
- [18] Rånby B G 1949 Aqueous colloidal solutions of cellulose micelles *Acta Chem. Scand.* **3** 649–50
- [19] Dufresne A 2013 Nanocellulose: a new ageless bionanomaterial *Mater. Today* **16** 220–7
- [20] Revol J F, Bradford H, Giasson J, Marchessault R H and Gray D G 1992 Helicoidal self-ordering of cellulose microfibrils in aqueous suspension *Int. J. Biol. Macromol.* **14** 170–2
- [21] Wang B and Walther A 2015 Self-assembled, iridescent, crustacean-mimetic nanocomposites with tailored periodicity and layered cuticular structure *ACS Nano* **9** 10637–46
- [22] de Vries H 1951 Rotatory power and other optical properties of certain liquid crystals *Acta Crystallogr.* **4** 219–26
- [23] Revol J-F, Godbout L and Gray D G 1998 Solid self-assembled films of cellulose with chiral nematic order and optically variable properties *J. Pulp Pap. Sci.* **24** 146–9
- [24] Kelly J A, Giese M, Shopsowitz K E, Hamad W Y and MacLachlan M J 2014 The development of chiral nematic mesoporous materials *Acc. Chem. Res.* **47** 1088–96
- [25] Hamad W Y and Hu T Q 2010 Structure-process-yield interrelations in nanocrystalline cellulose extraction *Can. J. Chem. Eng.* **88** 392–402
- [26] Shopsowitz K E, Qi H, Hamad W Y and MacLachlan M J 2010 Free-standing mesoporous silica films with tunable chiral nematic structures *Nature* **468** 422–5
- [27] Shopsowitz K E, Hamad W Y and MacLachlan M J 2011 Chiral nematic mesoporous carbon derived from nanocrystalline cellulose *Angew. Chem., Int. Ed. Engl.* **50** 10991–5
- [28] Lizundia E, Vilas J L and León L M 2015 Crystallization, structural relaxation and thermal degradation in Poly(l-lactide)/cellulose nanocrystal renewable nanocomposites *Carbohydr. Polym.* **123** 256–65
- [29] Liu D, Zhong T, Chang P R, Li K and Wu Q 2010 Starch composites reinforced by bamboo cellulosic crystals *Bioresour. Technol.* **101** 2529–36
- [30] Lin N and Dufresne A 2014 Surface chemistry, morphological analysis and properties of cellulose nanocrystals with gradiented sulfation degrees *Nanoscale* **6** 5384–93
- [31] Lizundia E, Nguyen T D, Vilas J L, Hamad W Y and MacLachlan M J 2017 Chiroptical luminescent nanostructured cellulose films *Mater. Chem. Front.* **1** 979–87

- [32] Giese M, Blusch L K, Khan M K, Hamad W Y and MacLachlan M J 2014 Responsive mesoporous photonic cellulose films by supramolecular cotemplating *Angew. Chemie—Int. Ed.* **53** 8880–4
- [33] Lizundia E, Nguyen T D, Vilas J L, Hamad W Y and MacLachlan M J 2017 Chiroptical, morphological and conducting properties of chiral nematic mesoporous cellulose/polypyrrole composite films *J. Mater. Chem. A* **5** 19184–94